Talanta 85 (2011) 2430–2436

Contents lists available at ScienceDirect

Talanta

journal homepage: www.elsevier.com/locate/talanta

On chip electrochemical detection of sarcoma protein kinase and HIV-1 reverse transcriptase

Sanela Martić, Mahmoud Labib, Heinz-Bernhard Kraatz*

Department of Chemistry, University of Western Ontario, 1151 Richmond Street, London, ON, Canada N6A 5B7

ARTICLE INFO

Article history:
Received 21 June 2011
Accepted 26 July 2011
Available online 3 August 2011

Keywords:
Electrochemistry
Bioanalytical chemistry
HIV-1 reverse transcriptase
Sarcoma protein kinase
Ferrocene
Bioorganometallics
Microchip

ABSTRACT

In this study, we report a new multiplexed microchip platform exploiting a peptide-modified gold surface and a labeled electrochemical approach. The significance of the presented methodology lies in its ability to test related analytes, such as protein kinases and human immunodeficiency virus (HIV) proteins, that operate under separate mechanisms using a single device without interference. The technology is based on an electrochemical dual sensing mode that can be tuned towards monitoring separately two biochemical events, a biochemical reaction and a direct analyte-receptor binding. The first recognition process is illustrated by a sarcoma-related (*Src*) protein kinase which catalyzes phosphorylation transfer of a ferrocenoyl–phosphoryl group, from the ferrocene-labeled adenosine triphosphate (Fc-ATP) co-substrate, to the surface-bound target peptide and induces a current response. On the other hand, HIV-1 reverse transcriptase (RT) protein binding to the surface-immobilized ferrocene-labeled target peptide is characterized by a modulation in the current intensity and peak potential. This proof-of-principle study is based on two different biosensing components and serves as a new platform for monitoring multiple analytes of interest. This allowed detection limits of 0.1 $\mu g\,mL^{-1}$ and 50 $pg\,mL^{-1}$ for *Src* kinase and HIV-1 RT, respectively. The miniaturization of the electrochemical protein assay will have an impact in disease detection and treatment.

1. Introduction

The 2007 report of the Joint United Nations and World Health Organization on HIV/AIDS showed that world-wide 30–36 million persons are infected with the human immunodeficiency virus (HIV) or are living with the acquired immune deficiency syndrome (AIDS) infection. Together with about 2.5 million new HIV infections and 2 million HIV-related deaths annually, HIV/AIDS remains a significant concern [1]. A number of methods have been developed for the detection of the human immunodeficiency virus (HIV) [2], including tests for HIV-1 or HIV-2 antibodies [3], viral RNA [4], and viral P24 assays [5], viral load analysis [6], and CD4+ T lymphocytes counting [7]. One has to stress that antibody-based assays are currently the gold standard for the detection of HIV infection *in vitro*. Progression of the infection and efficacy of antiviral treatments are evaluated by viral load analysis and CD4+ T lymphocyte counting [8].

Suitable targets are also HIV related enzymes, in particular those that are passed on from the virus to the CD4+ T lymphocytes and that are necessary for viral reproduction within the host cell. The absolute requirement of HIV-1 reverse transcriptase (RT) for HIV replication has made this enzyme one of the major targets for HIV detection and therapy. A number of techniques have been reported for RT detection, including one based on the polymerase chain reaction [9], on electrophoresis [10], on combined microbalance and mass spectrometry measurements [11], or use fluorescent tags [12]. Given the ongoing need for rapid analytics for viral enzymes that are sensitive, cheap, robust, simple to use, and require only minimal sample preparation, we have recently reported the use of an electrochemical assay for the detection of three HIV-1 enzymes [13,14].

Recently it was noted that the interplay between protein kinases and HIV-1 proteins drives the cellular function and expression and is involved in the progression of HIV disease [15]. In particular, the sarcoma-related (*Src*) protein kinase family members influence HIV-1 infection and virus transfer to autologous CD4+ T cells, while the HIV modulates the mitogen-activated protein kinases and *Src* kinases by inducing tyrosine phosphorylation [16]. For example, the kinase-catalyzed phosphorylations of the HIV-1 protease and HIV-1 RT induce the higher activities in HIV enzymes [17]. In turn, some HIV proteins can activate *Src* and turn on other kinases downstream, promoting the kinase overexpression that may lead to certain cancers. Most commonly, the HIV proteins bind *Src* family protein tyrosine kinases *via* interactions with their SH3 domains. For example, *Nef*, a protein that is required for high-titer viral replication, interacts with cellular

* Corresponding author. Tel.: +1 519 661 2166x81561; fax: +1 519 661 3022.
E-mail addresses: bkraatz@utsc.utoronto.ca, hkraatz@uwo.ca (H.-B. Kraatz).

0039-9140/$ – see front matter © 2011 Elsevier B.V. All rights reserved.
doi:10.1016/j.talanta.2011.07.090

kinase proteins, such as *Src*, because of their role in lymphocyte and macrophage signaling pathways [18]. A co-expression of *Nef* and protein kinase induces kinase activation and turns on cellular transformation [19,20], and is implicated in the pathogenesis of HIV/AIDS [21–24]. Presumably, *Src* kinases are potentially required for efficient HIV-1 replication. Studies suggest that redundant activation of *Src* occurs in HIV-infected cells and that the *Src* interactions with HIV proteins contribute to HIV-1 associated nephropathy, which is the most common cause of chronic renal failure in HIV-seropositive patients. Clearly, the relationship between the protein kinases and HIV-related proteins has relevant health implications in diagnostics and therapeutics. Because of the intimate nature of protein kinases and HIV proteins interactions, it is of interest to develop a sensing platform that combines HIV protein detection, such as HIV-1 RT, with the ability to also monitor *Src* activity. Rather than using a more conventional approach for multi-bioanalyte detection, we decided to develop an electrochemical microarray to monitor, on a single microchip, HIV-1 RT binding to a target ferrocene (Fc)-bioconjugate, in addition to the *Src*-catalyzed ferrocenyl-phosphorylation of peptide substrates on a surface [25,26]. At the heart of this report is the development of an electrochemical microarray that allows us to modify areas of the array with different biorecognition elements, selectively, for HIV-1 RT binding to a target peptide VEAIIRILQQLLFIH, or for monitoring *Src* phosphorylations of the target peptide EGIYDVP. The HIV-1 RT system is based on monitoring the modulation of the electrochemical signal of the immobilized Fc-VEAIIRILQQLLFIH conjugate, while the *Src* detection is essentially a signal ON sensor monitoring the appearance of the Fc redox current transferred to the target peptide by the *Src* protein kinase from the Fc-labeled adenosine triphosphate (Fc-ATP) conjugate. To our knowledge this is a first example of a device that encompasses two families of proteins, such as kinases and HIV, towards monitoring two independent biochemical events, and holds a great promise for monitoring disease onset and progression.

2. Materials and methods

2.1. Materials, reagents and general methods

HIV-1 RT was purchased from Applied Biosystems (Streetsville, ON, Canada). The HIV-1 RT-specific peptide (VEAIIRILQQLLFIH) and the protein kinase substrate peptide (EGIYDVP) were purchased from BioBasic Inc. (Markham, ON, Canada). Sarcoma related kinase (*Src*) was purchased from Cell Signaling. Ethanolamine and hexanethiol were purchased from Sigma–Aldrich (Canada). All other reagents were of analytical grade. Freshly distilled ethanol and the deionized water (18.2 MΩ cm resistivity) from a Millipore Milli-Q system were used throughout this work. All measurements were carried out at room temperature (25 °C). Adenosine 5′-[γ-ferrocenyl] triphosphate (Fc-ATP) was synthesized according to the procedure published elsewhere [27]. A lipoic-ferrocene-amino acid conjugate was synthesized from 1-aminoferrocene-1′-carboxylic acid using the literature coupling procedure [14,28]. Scanning electron microscopy (SEM) images were obtained using LEO 1540XB FIB/SEM model (Zeiss Germany) with an acceleration voltage of 1.0 kV or 20.0 kV and a magnification power of 28×, 463× and 1.01k×. TOF-SIMS experiments were performed with TOF-SIMS IV (ION-TOF GmbH, Munster, Germany), which was equipped with a Bi liquid metal ion source. For all measurements, a 25 keV Bi_3^+ cluster primary ion beam with a pulse width of 12 ns was employed (target current of ~1 pA). The cycle time for the process of bombardment and detection was 100 μs (or 10 kHz). A pulsed, low energy electron flood was used to neutralize sample charging. For each sample, spectra were collected from 128 × 128 pixels over an area of 190 μm × 190 μm for 60 s. Negative ion spectra were internally calibrated by using H^-, C^- and CH^- signals. All images were taken in the negative mode and collected from the raw data.

2.2. Microchip fabrication and packaging

For the preparation of patterned microchip electrodes, a deposition of silicon oxide (2 μm) was followed by the chromium (5 nm) onto the silicon wafer (500 μm). Photolitography was used for patterning the gold layer (200 nm) on the surface. Finally, an insulating layer of Shipley 1813 photoresist was spin deposited over the entire wafer to a thickness of 2.2 nm. The 10 μm diameter electrodes are exposed and developed through the photoresist layer down to the gold conductive electrode. Similarly, the gold pads (1 mm^2) were exposed as connections for electrochemical measurements. The phororesist was hard baked on a hot plate for 30 min at 120 °C. To prevent contamination of the electrodes, a protective photoresist layer was spin-deposited over the entire wafer and soft baked at 95 °C for 2 min. The wafer, containing 20–30 individual arrays was diced into chips and the top photoresist was removed, leaving the insulating photoresist layer and electrode layer intact. The photoresist was not sensitive to the reagents for the electrochemical measurements. In addition, the photoresist is also persistent over the potential range from −0.2 to 1.5 V versus Ag/AgCl. A scanning electron microscopy (SEM) images of the electrode wells are shown in the Supplementary data. After patterning, the silicon wafer was cut into squares (1 cm × 1 cm) prior to gold wire bonding. The gold wire bonding for connecting the microchip pads to the package was performed at the Nanofabrication Facility at The University of Western Ontario. The microchip package and socket were purchased from Chelsea technologies (USA). One end of this gold wire was centered on the package lead, the other end was connected with one of eight gold pads (1 mm^2). The microwires were each separated by 50 μm. The microchip/package assembly is depicted in the Supplementary data.

2.3. Microchip cleaning and electrochemical microchip characterization

Before proceeding with the preparation of the biorecognition surface, the chip was cleaned thoroughly by ultrasonication in water (5 min), followed by sonication in freshly distilled ethanol to reduce any gold oxide (20 min). The microchip was dried under inert N_2 atmosphere. The electrical connectivity of the final device was probed by using the assembled device and the standard electrochemical set-up in the presence of a well known redox probe, a ferric/ferrocyanide redox couple (5 mM $K_4[Fe(CN)_6]\cdot 3H_2O$ and $K_3[Fe(CN)_6]\cdot 3H_2O$ in milliQ water containing 50 mM KNO_3 as a supporting electrolyte). The specific surface area was determined by using cyclic voltammetry and from the scan rate dependent current of the solution redox probe. The current dependence on the square root of the scan rate for the $[Fe(CN)_6]^{3-/4-}$ redox pair was observed. The linearity of the oxidation and reduction current suggested that the redox reaction was a diffusion-controlled process. From the Randles–Sevcik equation [29,30] of the slope of the current versus the square root of the scan rate, the working surface area of the gold microelectrode was calculated. Under the following assumptions, the diffusion coefficient, D, of 6.6×10^{-6} cm^2 s^{-1}, a working concentration, c, at 5 mM and one-electron process at the gold electrode for the $[Fe(CN)_6]^{3-/4-}$ redox pair, the microelectrode radius and the specific surface area were determined to be 9.5 μm and 280 μm^2, respectively. Furthermore, the intraquadrant and interquadrant reproducibility on the microchip was tested in the presence of $[Fe(CN)_6]^{3-/4-}$ redox couple. Firstly, the intraquadrant current intensity for a group of 4 independent electrodes within a quadrant was evaluated and the reproducibility was

estimated to be in the 90–95% range. Subsequently, an interquadrant current was tested for 4 selected electrodes between 4 quadrants and the current reproducibility was found to deviate from 5–30%. With regards to the intra- or interquadrant current amplitudes, the microchip device is characterized with a relatively high reproducibility and stability and was used for testing of different types of analytes.

2.4. Preparation of peptide-modified microchip

Separate quadrants of the chip were spotted with different chemistries that allowed us to attach different biorecognition elements to the set of four 10 μm gold electrodes in the quadrant. For this purpose, different quadrants of a clean microchip were spotted with: (a) 5 μL solution of 2 mM *N*-succinimide lipoic acid ester in ethanol and (b) 5 μL solution of 2 mM lipoic acid-ferrocene amino acid conjugate in ethanol for 24 h at room temperature. This formed a sublayer on the gold electrodes that was further modified with a specific biorecognition element. The solutions were separated using the in-house built rubber membrane and the microchip housing. Afterwards, the microchip was rinsed with ethanol and dried under N_2 atmosphere.

Next, the quadrants were modified further to attach specific biorecognition elements. To the quadrant previously spotted with the lipoic acid-ferrocene amino acid conjugate, a solution of 1:1 mixture of 1-ethyl-3-(3-dimethylaminopropyl)carbodiimide (EDC) and *N*-hydroxysuccinimide (NHS) (10 mM each in 5 μL water) was added allowing the activation of the carboxylic acid group. After 1 h, a solution of the HIV RT-specific peptide (VEAIIRILQQLLFIH, 5 μL of 1 mM peptide in 10 mM sodium phosphate buffer, pH 7.4) was added and left to incubate overnight at 4 °C.

To the quadrant previously spotted with *N*-succinimide lipoic acid ester, the *Src* kinase substrate peptide EGIYDVP was added (5 μL aqueous solution of 100 μM peptide) and left to incubate over night at 4 °C.

Any unreacted active ester on the gold electrode array was blocked with an ethanolic solution of 100 mM ethanolamine for 1 h at room temperature. Subsequently, the chip was treated with 10 mM hexanethiol to back-fill the Au surface and to minimize pinholes. Finally, the electrode array was rinsed with ethanol and Millipore water to give the peptide-modified sensor surface.

2.5. Protein protocols

Two different chemical environments are necessary to maximize the phosphorylation activity of the protein kinase *Src* and binding of HIV-I RT to its respective peptide target on the same microchip.

(a) One quadrant modified with the *Src* target peptide EGIYDVP linked to the four gold spots in the quadrant was loaded with the assay buffer (5 mM 3-(*N*-morpholino)propanesulfonic acid (MOPS) pH 7.5, 2.5 mM β-glycerophosphate, 1 mM ethylene glycol tetraacetic acid (EGTA), 0.4 mM ethylenediamine tetraacetic acid (EDTA), 2.5 mM $MnCl_2$ and 4 mM $MgCl_2$). The total volume of the assay buffer was 5 μL, containing also *Src* kinase (1 μg mL^{-1}) and Fc-ATP (200 μM). After 2 h of incubation at 37 °C in a heating block, the microchip was washed using 0.1 M sodium phosphate buffer, pH 7.4, prior to measurement. A positive control experiment was carried out on a second quadrant, on the same chip, in the presence of Fc-ATP but in the absence of *Src* kinase.

(b) For the purpose of HIV-1 RT study, the third quadrant of the microchip was spotted with 5 μL solution of 100 pg mL^{-1} HIV-1 RT in water at 37 °C for 2 h in a heating block. The microchip was rinsed with 0.1 M sodium phosphate buffer (pH 7.4) prior to all electrochemical measurements. On the fourth quadrant, a positive control was carried out in the absence of HIV-1 RT.

Furthermore, the protein concentration studies were performed by varying the amounts of *Src* kinase (0, 0.2, 0.5, 1 and 2 μg mL^{-1}) and HIV-1 RT protein (0, 100, 750, 1000 and 1500 pg mL^{-1}) on two separate chips.

2.6. Electrochemical measurements

All electrochemical studies (cyclic voltammetry (CV) and square wave voltammetry (SWV)) were performed with an electrochemical analyzer (CH Instruments 660B, TX, USA). A conventional three-electrode system was used with individual peptide-modified gold microelectrodes of the microchip as working electrodes, a platinum wire as a counter electrode, and Ag/AgCl 3 M KCl (CHI Instruments) as a reference electrode. The reference electrode was always isolated from the cell by a miniature salt bridge (agar plus KNO_3). The electrochemical setup is depicted in the Supplementary data. All electrochemical measurements were performed in 0.1 M sodium phosphate buffer at pH 7.4. All CV experiments were performed at a scan rate of 100 mV s^{-1} in the potential range of 0–600 mV or 200–600 mV vs Ag/AgCl, unless otherwise mentioned. SWV experiments were carried out in the same range with a step potential of 5 mV, pulse amplitude of 25 mV, and a frequency of 15 Hz. For investigation of microchip electrochemical characteristics and the blocking studies, 5 mM solution of $K_4[Fe(CN)_6]\cdot 3H_2O$ and $K_3[Fe(CN)_6]\cdot 3H_2O$ in water containing 50 mM KNO_3 was used and the electron transfer kinetics of the $[Fe(CN)_6]^{3-/4-}$ redox reactions were investigated after each modification step in biosensor design.

3. Results and discussion

3.1. Microchip design and device fabrication

The modification of the chip involves the sequential deposition of the silicon dioxide, chromium and gold layers on the silicon wafer. The sputtering chromium layer acts as the adhesion layer for Au. Photolithography was used for the microchip patterning as illustrated in Fig. 1A. The microchip (actual size 1 cm × 1 cm) consists of 16 microelectrodes each with a diameter of 10 μm, grouped into four distinct quadrants located at each of the corners, which allows different chemistries in different quadrants, facilitates manual handling and solvent additions, while at the same time allowing data acquisition from four electrodes in the quadrant to give statistically meaningful results (see Fig. 1A inset). The calculated surface area of each electrode was 280 μm^2.

The microchip surface was characterized by scanning electron microscopy (SEM) and the image in Fig. 1B shows four distinct 10 μm gold microelectrode pads in the center of a larger substructure. In the presence of the $[Fe(CN)_6]^{3-/4-}$ redox couple, each of the gold microelectrodes displays current response that is in accordance with the electrode size (Fig. 1C). Imaging time-of-flight secondary ion mass spectrometry (Fig. 1D) clearly shows signals due to solvent accessible 10 μm gold microelectrode spots. The remainder of the microchip is protected by photoresist.

The microchip has 16 independent and individually addressable electrodes, which are connected to commercially available package housing *via* wire bonding. The wire-bonded microchip/package unit was mounted onto a commercially available socket. The assembled device was connected to a potentiostat *via* conducting socket pins at the bottom of the socket, which allows the measurement of each electrode separately. Electrochemical measurements were performed using the device in a typical 3-electrode set-up

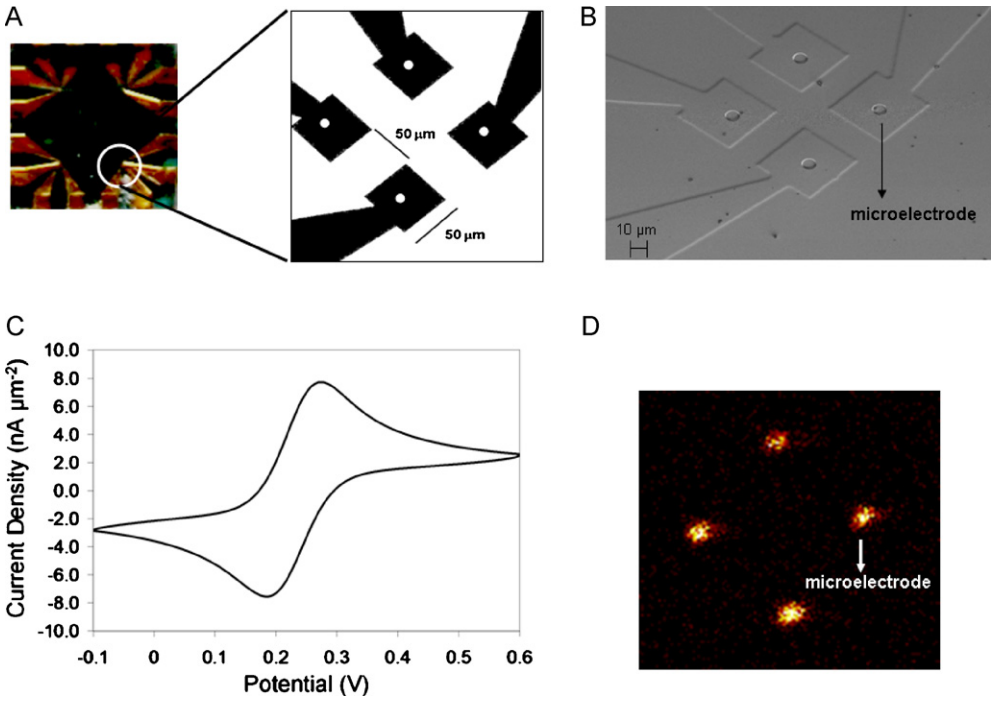

Fig. 1. Photograph of (A) microchip and the inset showing four distinct microelectrodes within the microchip quadrant. (B) SEM image of the single quadrant showing four distinct microelectrodes. (C) Cyclic voltammogram of the bare gold microelectrode in the presence of 5 mM $[Fe(CN)_6]^{3-/4-}$ solution redox pair (50 mM KNO_3) at a scan rate 100 mV s^{-1}. (D) TOF-SIMS image showing a negative mode Au intensity from a representative quadrant containing four 10 μm microelectrodes. The bright spots correspond to the Au intensity with a total field of view of 190 μm × 190 μm.

as shown in the Supplementary data with an external platinum wire as counter electrode. An Ag/AgCl reference electrode was connected to the device by a salt bridge.

3.2. Multi-protein detection

The basic biosensing principle for the *Src* and HIV-1 RT proteins on a chip is shown in Fig. 2. The biorecognition elements for both targets were build up in a stepwise fashion on the chip, as outlined in the experimental section, starting from an active ester film on a Au surface followed by reaction with the respective peptide making up the biorecognition element (a). Fig. 2A shows the sensor scheme for *Src* protein kinase in one of the quadrants of the chip, consisting of the target peptide with the sequence EGIYDVP, which is Fc-phosphorylated by *Src*. In the presence of Fc-ATP, *Src* transfers a ferrocenyl-phosphate to the tyrosine (Y) of the surface bound peptide, making it possible to detect and quantify the redox active Fc group (b).

In the second quadrant of the chip, the chemistry selective for HIV-1 RT is based on the lipoic acid-Fc amino acid conjugate followed by coupling to the target peptide VEAIIRILQQLLFIH (Fig. 2B). Detection in this case is based on the modulation of the electrochemical properties of the surface bound Fc group due to HIV-1 RT binding to the peptide sequence, thereby altering the electrochemical properties of the Fc probe (b).

For the *Src* kinase detection, the short peptide with EGIYDVP sequence serves as the reaction substrate for a transfer of γ-ferrocenoyl phosphate group from Fc-ATP to the tyrosine residue of the surface bound peptide (Fig. 2A). The transfer of the redox probe to the surface results in a measurable current response. *Src* protein kinase-catalyzed phosphorylation reaction on the surface was characterized by the formal potential, E^0, at ~410 mV, a potential difference, ΔE, at 60 mV and an i_{pa}/i_{pc} ratio at 0.9. Cyclic voltammograms (Fig. 3A) and square-wave voltammograms (Fig. 3B) indicate quasi-reversible oxidation characteristic of a ferrocene group [31]. The electrochemical parameters suggest an efficient electron-transfer process for Fc-phosphopeptides on the surface. Additional studies reveal a current dependence on the scan rates (20–300 mV) and the linear dependence of the anodic and cathodic currents on the same [31]. The trend is associated with the surface-bound redox probe that excludes a diffusion-controlled process. The positive control experiment performed in the absence of *Src* kinase reveals negligible current activity (a) and indicates that kinase-catalyzed phosphorylation is required for the observed current. Moreover, the biosensing surface is characterized by a minimal non-specific adsorption. Concentration of *Src* kinase was varied in order to investigate the effect of the protein kinase concentration on the analytical response and to determine the dynamic range of the biosensor. The results suggest that the detection of *Src* protein kinase is at the nanogram level wherein the saturation of the biosensor surface was achieved at ~1 μg mL^{-1} *Src* kinase concentration. A linearity of the current density versus *Src* concentration was maintained in the 0.2–2 μg mL^{-1} range (R^2 = 0.9836), and the limit of detection was estimated to be ~0.1 μg mL^{-1}.

Unlike in the protein kinase assay wherein the redox signal is related to biochemical process which induces a signal ON response, in the HIV assay the analytical signal is modulated in the presence of the HIV-1 RT protein. A lipoic-Fc amino acid conjugate, a disulfide analogue of ferrocene, serves as the capture probe for target peptide and in turn for target protein. In Fig. 4A and B, an immobilized lipoic-Fc amino acid conjugate (a) yields a one-electron reversible redox behaviour that is characteristic of ferrocene group. The system is characterized by the formal potential, E^0, at ~260 mV, a potential difference, ΔE, at 70 mV and an i_{pa}/i_{pc} ratio at 0.9 [31]. The redox active layer is characterized by a current dependence on the scan rate and a linear dependence of the anodic and cathodic currents with respect to the scan rates (20–200 mV) [32]. Subsequent immobilization of a target peptide VEAIIRILQQLLFIH (1 mM), which is highly specific for HIV-1 RT protein, leads to slight reduction of current intensity (b). Furthermore, blocking of activated

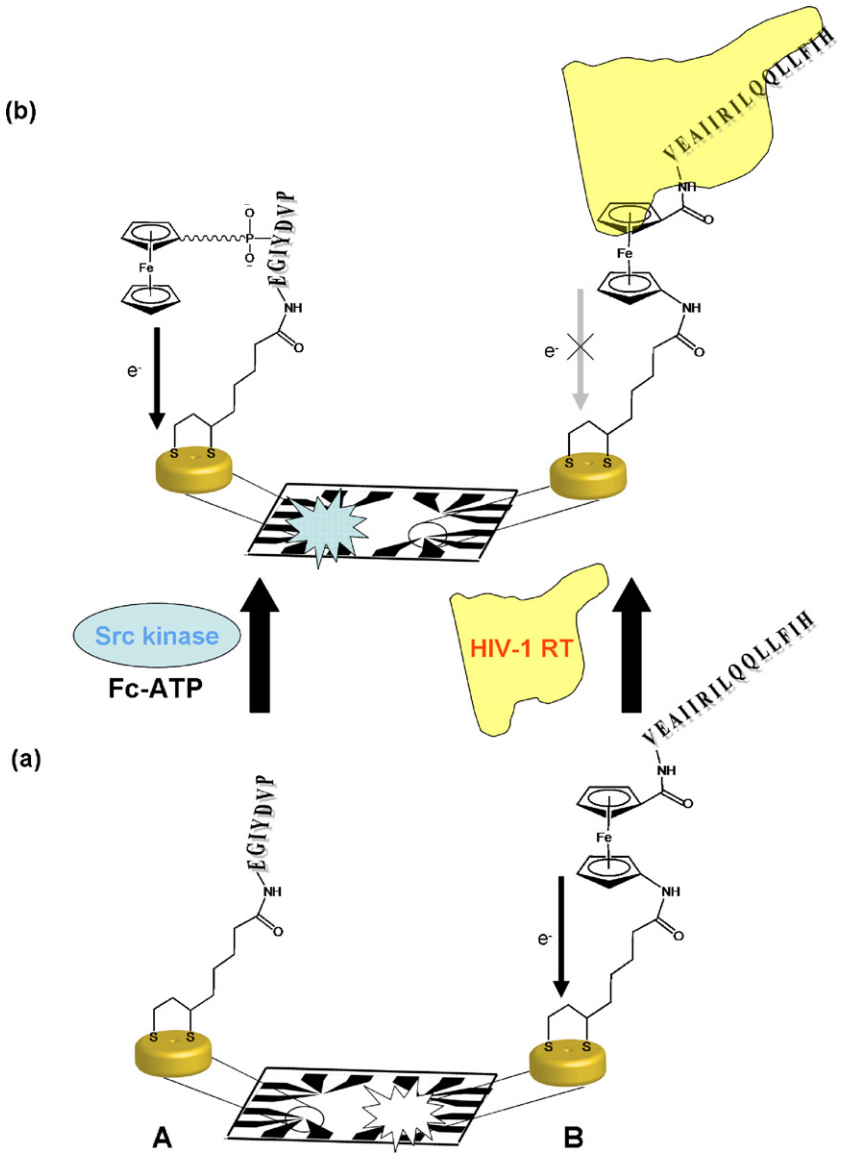

Fig. 2. Illustration of the dual peptide-biosensor surfaces for sensory pathways A and B. (A) An *N*-succinimide lipoic acid ester immobilized on Au electrode followed by amide coupling to a target peptide EGIYDVP (a). The addition of protein analyte *Src* kinase in the presence of Fc-ATP co-substrate leads to the Fc-phosphorylation and produces an electrochemical signal (b). (B) A lipoic-Fc-amino acid immobilized on Au electrode followed by coupling to a target peptide VEAIIRILQQLLFIH in the presence of EDC and NHS (a). The addition of analyte HIV-1 RT protein to platform B produces the current modulation and signal reduction (b). Prior to the analyte addition (a), the platform B is characterized by a strong redox activity but platform A is electrochemically silent.

NHS-ester groups with 100 mM ethanolamine and back-filling of Au electrode with 10 mM hexanethiol were necessary to avoid non-specific binding of proteins (c). A ready-to-go biosensor was then used for the detection of HIV-1 RT protein. In the presence of 100 pg mL^{-1} HIV-1 RT, it is evident form the CVs and SWVs that protein addition to the peptide target results in a decrease in the current intensity and a slight cathodic shift to ~290 mV (d). Modulation of the redox signal can be caused by changes in the accessibility of the redox probe to the electrode surface [33–35], or by a partial encapsulates of the Fc label upon binding of HIV-1 RT to the peptide conjugate preventing efficient access of counter ions to the Fc group [28]. This is in a big contrast to the electrochemical response observed for protein kinase, wherein the surface-assisted biochemical reaction induces the redox activity. In the case of HIV-1 RT protein assay, the protein binding modulates the existing electrochemical response. HIV-1 RT concentration was varied in order to estimate the effect of analyte on the current density and the redox potential. As shown in Fig. 4C, reduction in current density was observed after addition of 100 pg mL^{-1} HIV-1 RT and continued to decrease with further addition of the protein. Notably, the HIV-1 RT concentrations in the nanogram range were outside the dynamic range of the biosensor. A slight anodic shift in the redox potential, ΔE, was observed upon addition of HIV-1 RT from ~280 V to 310 V which represents an additional signature feature of the developed assay. A linear relationship between current density and HIV-1 RT concentration was observed in 100–1000 pg mL^{-1} range (R^2 = 0.9794), and the limit of detection was estimated to be ~50 pg mL^{-1}.

The microchip platform allows for the analyte detection with moderate intraquadrant reproducibility (60–80%) and interquadrant reproducibility (70–90%) for a specific protein. We demonstrated a reproducible response for *Src* and HIV-1 RT proteins on a single device, and a linear response over a two order of magnitude range of *Src* concentration and in a picogram range for

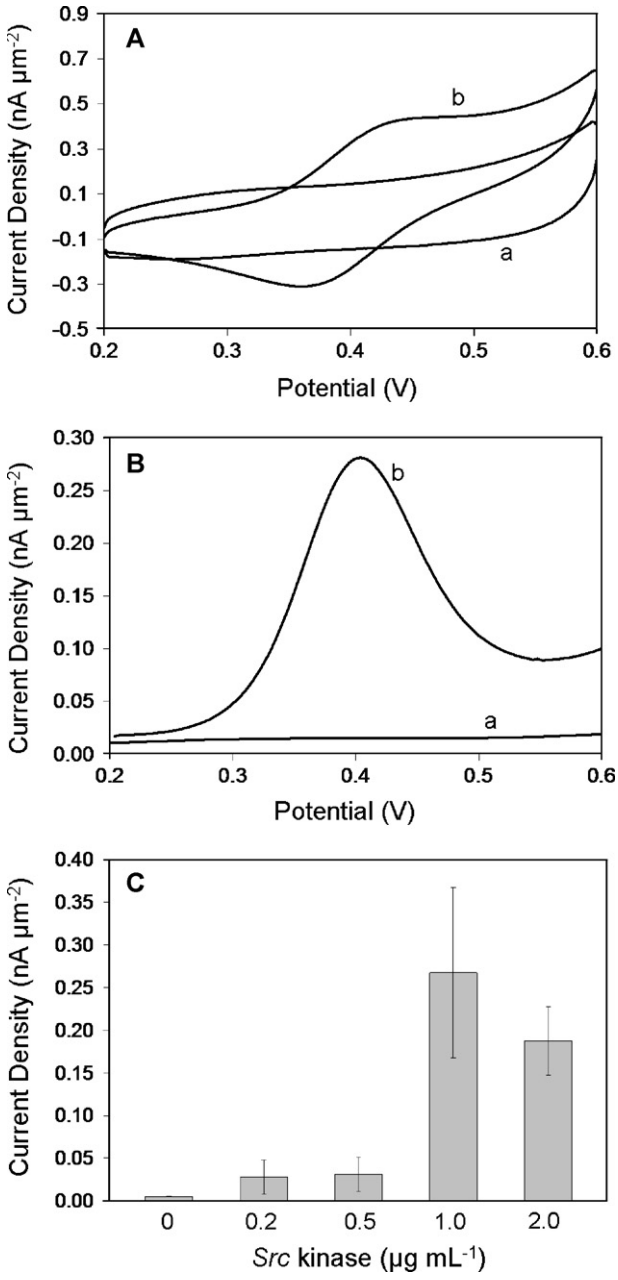

Fig. 3. (A) Cyclic voltammograms and (B) square-wave voltammograms in the absence (a) and in the presence of *Src* kinase (b). (C) Current density as a function of *Src* kinase concentrations: 0.2–2 µg mL^{-1}. 0.1 M sodium phosphate buffer, pH 7.4 (current density was estimated from the normalized SWVs and the error bars represent measurements at 4 separate electrodes).

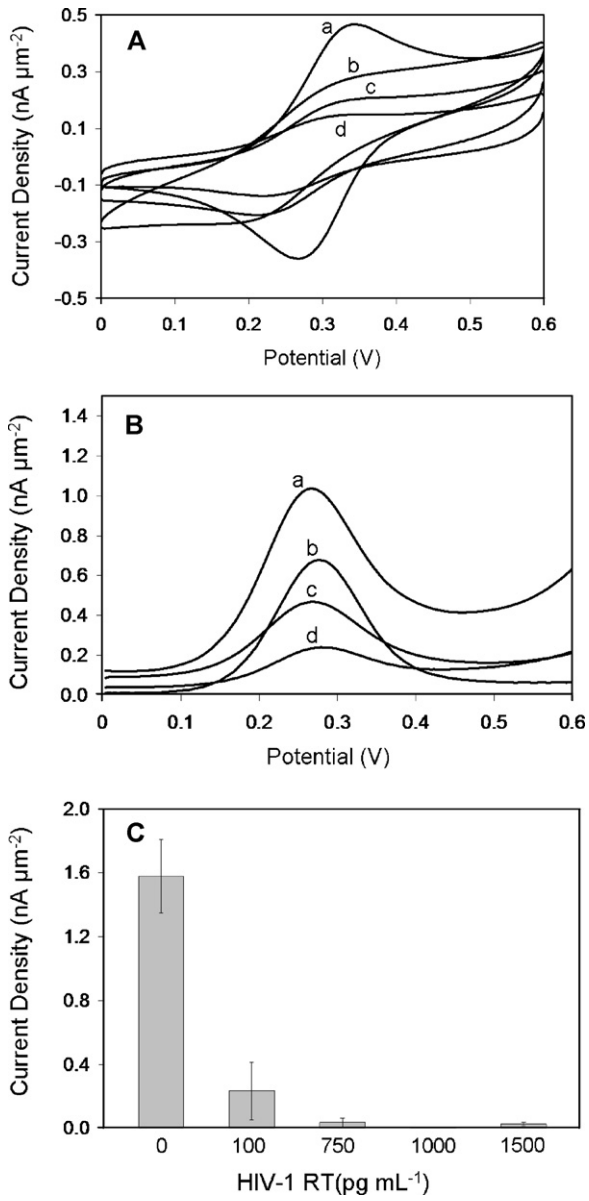

Fig. 4. (A) Cyclic voltammograms and (B) square-wave voltammograms of the biosensor after (a) lipoic-ferrocene amino acid conjugate, (b) incubation of peptide VEAIIRILQQLLFIH, (c) blocking with ethanolamine and back-filling with hexanethiol, and (d) addition of HIV-1 RT (100 pg mL^{-1}). (C) Plot of current density as a function of HIV-1 RT concentrations: 0–1500 pg mL^{-1}. 0.1 M sodium phosphate buffer, pH 7.4 (current density was estimated from the normalized SWVs and the error bars represent measurements at 4 separate electrodes).

HIV-1 RT, respectively. Currently, the microchip design and fabrication are being optimized to achieve integrated counter/reference electrode set-up and an improved reproducibility. Given the specific mode of action for the two studied proteins, the minimal cross-reactivity is expected. Notably, only a single peak potential was observed in a given assay. Presumably, the HIV-1 RT protein does not catalyze the phosphorylation reaction and the *Src* protein kinase is unlikely to phosphorylate the VEAIIRILQQLLFIH peptide sequence due to the lack of tyrosine, serine or threonine residues. Alternatively, the two distinct peak potentials, ~410 and 260 mV for kinase assay and HIV-1 assay, respectively, may potentially be used to monitor multiple-protein activities in complex mixtures.

A distinguishing feature of the integrated biosensor is the incorporation of two sensing platforms for targeting the protein–peptide interactions in two distinct environments. A dual sensing mode allows for a distinct electrochemical signal as a direct result of bioprocesses on the surface and alternative redox response upon surface-assisted protein–peptide complex formation. Though the existing study demonstrates detection of two inter-related proteins in their purified form, the methodology has great potential for extending the sensing components to monitor early phosphorylation events or an infection during the course of HIV disease. Because of the biochemical link between the protein kinases and HIV enzymes with high impact in disease detection and treatment, the potential value of the methodology presented herein cannot be ignored. We are currently working on optimizing the electro-

chemical interface to meet the requirements for multiple analytes detection *in vitro*.

4. Conclusion

We presented a multiplexed microchip array based on the peptide-immobilized microelectrodes for the purpose of monitoring two types of inter-related proteins, *Src* protein kinase and HIV-1 reverse transcriptase on a single device. The dual methodology uses a redox-labeled approach to monitor enzymatic reactions and protein binding, simultaneously. The microchip platform is a useful tool for studying multiple analytes of interest, that operate under different mechanisms, and we are currently extending the multiplexed sensing towards detection of a variety of protein kinases and HIV-related enzymes in complex mixtures. In addition, the microchip technology is currently being optimized and statistically evaluated.

Acknowledgements

S. Martić is grateful to the Ontario Ministry of Research and Innovation and the University of Western Ontario for funding. The authors are also thankful to Tim Goldhawk and Dr. Todd Simpson of Western's Nanofabrication facility for microchip manufacturing. This work was supported by operating grants from the Natural Sciences and Engineering Research Council of Canada (NSERC) and the Western Innovation Fund (WIF).

Appendix A. Supplementary data

Supplementary data associated with this article can be found, in the online version, at doi:10.1016/j.talanta.2011.07.090.

References

[1] http://data.unaids.org/pub/epislides/2007/2007_epiupdate_en.pdf.
[2] D.D. Richman, Nature 410 (2001) 995–1001.
[3] B. Feng, Y. Dai, H. Zhang, L. Wang, Y. Ding, H. Zeng, Immunoassay Immunochem. 30 (2009) 457–466.
[4] J. Müller, Methods Mol. Biol. 630 (2010) 319–335.
[5] P. Brown, Nature 405 (2000) 263.
[6] C. Torti, G. Lapadula, F. Maggiolo, S. Casari, F. Suter, L. Minoli, C. Pezzoli, M.D. Pietro, G. Migliorino, E. Quiros-Roldan, N. Ladisa, L. Sighinolfi, F. Gatti, G. Carosi, HIV Clin. Trials 8 (2007) 112–120.
[7] M. Cavrois, C. de Noronha, W.C. Greene, Nat. Biotechnol. 20 (2002) 1151–1154.
[8] X. Jiang, M.G. Spencer, Biosens. Bioelectron. 25 (2010) 1622–1628.
[9] H. Zhang, Z. Wang, X.F. Li, X.C. Le, Angew. Chem. Int. Ed. 45 (2006) 1576–1580.
[10] H. Zhang, X.F. Li, X.C. Le, J. Am. Chem. Soc. 134 (2008) 34–35.
[11] T.M.A. Gronewold, A. Baumgartner, J. Hierer, S. Sierra, M. Blind, F. Schäfer, J. Blümer, T. Tillmann, A. Kiwitz, R. Kaiser, M. Zabe-Kühn, E. Quandt, M. Famulok, J. Prot. Res. 8 (2009) 3568–3577.
[12] J.F. Krebs, A.R. Kore, Bioconjug. Chem. 19 (2008) 185–191.
[13] M. Labib, P.O. Shipman, S. Martic, H.-B. Kraatz, Analyst 136 (2011) 708–715.
[14] M. Labib, P.O. Shipman, S. Martic, H.-B. Kraatz, Electrochim. Acta 56 (2011), 5122–5122.
[15] C. Gilbert, C. Barat, R. Cantin, M.J. Tremblay, J. Immunol. 178 (2007) 2862–2871.
[16] R.K. Ganju, N. Munshi, B.C. Nair, Z.-Y. Liu, P. Gill, J.E. Groopman, J. Virol. 72 (1998) 6131–6137.
[17] E. Haneda, T. Furuya, S. Asai, Y. Morikawa, K. Ohtsuki, Biochem. Biophys. Res. Commun. 275 (2000) 434–439.
[18] S.D. Briggs, E.C. Lerner, T.E. Smithgall, Biochemistry 39 (2000) 489–495.
[19] S.D. Briggs, T.E. Smithgall, J. Biol. Chem. 274 (1999) 26579–26583.
[20] S.D. Briggs, M. Sharkey, M. Stevenson, T.E. Smithgall, J. Biol. Chem. 272 (1997) 17899–17902.
[21] R.P. Trible, L. Emert-Sedlak, T.E. Smithgall, J. Biol. Chem. 281 (2006) 27029–27038.
[22] K. Saksela, G. Cheng, D. Baltimore, EMBO J. 14 (1995) 484–491.
[23] S. Arold, P. Franken, M.P. Strub, F. Hoh, S. Benichou, R. Benarous, C. Dumas, Structure 5 (1997) 1361–1372.
[24] S. Arold, R. O'Brien, P. Franken, M.P. Strub, F. Hoh, C. Dumas, J.E. Ladbury, Biochemistry 37 (1998) 14683–14691.
[25] B.T. Houseman, J.H. Huh, S.J. Kron, M. Mrksich, Nat. Biotechnol. 20 (2002) 270–274.
[26] S. Martic, M. Labib, H.-B. Kraatz, Analyst 136 (2011) 107–112.
[27] H. Song, K. Kerman, H.-B. Kraatz, Chem. Commun. (2008) 502–503.
[28] K.A. Mahmoud, H.-B. Kraatz, Chem. Eur. J. 13 (2007) 5885–5895.
[29] J.E.B. Randles, Trans. Faraday Soc. 44 (1948) 327–338.
[30] A. Sevcik, Collect. Czech. Chem. Commun. 13 (1948) 349–377.
[31] E. Laviron, in: A.J. Bard (Ed.), Electroanalytical Chemistry, vol. 12, Marcel Dekker, New York, 1982, pp. 53–157.
[32] C. Fan, K.W. Plaxco, A.J. Heeger, Proc. Natl. Acad. Sci. U.S.A. 100 (2003) 9134–9137.
[33] F. Ricci, R.Y. Lai, K.W. Plaxco, Chem. Commun. 36 (2007) 3768–3770.
[34] F. Ricci, R.Y. Lai, A.J. Heeger, K.W. Plaxco, J.J. Sumner, Langmuir 23 (2007) 6827–6834.
[35] S.E. Creager, T.T. Wooster, Anal. Chem. 70 (1998) 4257–4263.